Muon Capture in He^3†*

DOUGLAS R. CLAY,‡ JACK W. KEUFFEL, AND RICHARD L. WAGNER, JR.§
University of Utah, Salt Lake City, Utah

AND

RICHARD M. EDELSTEIN
Carnegie Institute of Technology, Pittsburgh, Pennsylvania

(Received 18 June 1965)

The rate has been measured for capture of negative muons on He^3 to form bound H^3. The monoenergetic recoil triton was observed in a He^3 gas scintillation target counter, and the rate was normalized to μ-decay electrons observed in surrounding counters. Triton pulses were analyzed in the two dimensions of energy and time with respect to the stopping muon, and with an ultimate energy resolution of 15%, full width at half-maximum, a clean separation could be made between recoil tritons and other muon-associated events. The measured capture rate is 1465 ± 67 sec^{-1}, in good agreement with other experiments and with predictions based on the "standard" theory of muon capture. Simultaneous limits were calculated for the vector and induced pseudoscalar coupling constants, $g_V{}^\mu$ and $g_P{}^\mu$, using the results of this experiment and of the experiments on muon capture in liquid hydrogen. These are $0.7<g_V{}^\mu/g_V{}^\beta<1.2$ and $1<g_P{}^\mu/g_A{}^\mu<17$ with central values of 0.99 and 11.6, respectively.

I. INTRODUCTION

THE muon capture process continues to be the least well understood of the three non-strangeness-changing weak interactions. Aside from the difficulties associated with a given experiment, and certainly they are not inconsiderable, the interpretation of experiments has in general been obscured by complicated nuclear-physics problems. In the case of muon capture in He^3, the experiment discussed in this paper, the nuclear-physics problems are minimal. Therefore, its result yields precise information about the capture process.

There are, however, four real interaction constants in the so-called standard theory[1] of muon capture. Since the present experiment measures only one specific combination of these constants, other information is required either in the form of assumptions about the universality of the Fermi interaction or the results of other experiments, or both.

The standard theory starts with the V–A theory of Feynman and Gell-Mann.[2] It is assumed that time-reversal invariance holds, but the two "second class" terms which Weinberg[3] has discussed are not included, although possibly they should be. The values of three of the constants, the vector g_V, the axial vector g_A, and the weak magnetism g_M, are predicted on the assumption of a universal Fermi interaction with conserved vector current CVC, and, hence, derive from measurements of β decay and electron scattering.[1,4] The fourth, the induced pseudoscalar constant g_P, has been calculated by Goldberger and Treiman[5] and by Wolfenstein.[6]

The many capture experiments which have been performed to date have generally been in good agreement with the standard theory. Yet, as has been mentioned, generally the theoretical predictions are not exact. There are, however, three experiments involving the capture process for which the uncertainty in the prediction is no more than a few percent:

1. The ratio of the rates for the processes $\pi^+\rightarrow e^+ + \nu$ and $\pi^+\rightarrow \mu^+ + \nu$.[7] This experiment demonstrates that $g_A{}^\mu(q^2)=g_A{}^\beta(q^2)(1.0\pm0.01)$, where $q^2=-m_\pi{}^2$.

2. Muon capture in liquid hydrogen. The reaction rate has been measured by three groups whose results are in good agreement.[8] The earlier discrepancy between the standard theory and the experimental values appears now to have been resolved by several authors[9] who have recalculated the muon-molecular wave func-

† Research supported in part by the National Science Foundation (University of Utah) and the U. S. Atomic Energy Commission (Carnegie Institute of Technology).

* Earlier reports of this experiment appear in Brookhaven National Laboratory Report BNL 837 (C-39), 1963 (unpublished), p. 303; R. L. Wagner, Jr., thesis, University of Utah, 1963 (unpublished); and D. R. Clay, thesis, University of Utah, 1964 (unpublished).

‡ Present address: Bell Telephone Laboratories, Murray Hill, New Jersey.

§ Present address: Lawrence Radiation Laboratory, University of California, Livermore, California.

[1] H. Primakoff, Rev. Mod. Phys. **31**, 802 (1959). For recent revues of the muon capture problem, see T. Ericson, *International Conference on High Energy Physics, Dubna, 1964* (Atomizdat, Moscow, 1965); H. Primakoff, *Course XXXII, International School of Physics, "Enrico Fermi"* (Academic Press Inc., New York, to be published); G. Feinberg and L. Lederman, Ann. Rev. Nucl. Sci. **13**, 431 (1963); and L. Wolfenstein, Brookhaven National Laboratory Report BNL 837 (C-39), 1963, p. 292 (unpublished).

[2] R. P. Feynman and M. Gell-Mann, Phys. Rev. **109**, 193 (1958).

[3] S. Weinberg, Phys. Rev. **112**, 1375 (1958).

[4] A. Fujii and H. Primakoff, Nuovo Cimento **12**, 327 (1959).

[5] M. L. Goldberger and S. B. Treiman, Phys. Rev. **111**, 354 (1958).

[6] L. Wolfenstein, Nuovo Cimento **8**, 882 (1958).

[7] E. Di Capua, R. Garland, L. Pondrum, and A. Strelzoff, Phys. Rev. **133**, B1333 (1964); H. L. Anderson, T. Fujii, R. H. Miller, and L. Tau, Phys. Rev. **119**, 2050 (1960).

[8] J. E. Rothberg *et al.*, Phys. Rev. **132**, 2664 (1963); R. H. Hildebrand and J. H. Doede, *Proceedings of the 1962 Annual International Conference on High Energy Physics at CERN* (CERN Scientific Information Service, Geneva, Switzerland, 1962), p. 418; E. Bertolini *et al.*, *ibid.* p. 421.

[9] W. R. Wessel and P. Phillipson, Phys. Rev. Letters **13**, 23 (1964); A. Halpern, *ibid.* **13**, 660 (1964); P. K. Kabir, Phys. Letters **14**, 257 (1965).

tion for the initial system from which the muon is captured.

3. The reaction of the present experiment, $\mu^-+He^3 \rightarrow H^3+\nu$, wherein the transition rate to the ground state of H^3 is measured by observing the monoenergetic recoil tritons. The reaction was first observed by Falomkin *et al.*,[10] in a diffusion cloud chamber. Another experiment, using a gas scintillator technique similar to ours, has been performed by Auerbach *et al.*[11] The reaction rate for this process was first calculated by Fujii and Primakoff,[4] and Werntz.[12] The precision of the calculation is enhanced by several favorable circumstances. The transition from one "trion" to the other is superallowed (they form an isotopic spin doublet) and use can be made of the ft value for triton β decay, the inverse process. Since the trions are small, the deviation from the prediction for point nuclei is only $\sim 30\%$. Furthermore, much is now known about the trion form factors from extensive electron-scattering data[13] as analyzed by Schiff[14] and others. Several authors[15,16] have recently recalculated the rate making use of the scattering data, and the finite-size correction is well enough understood so that the over-all error in the theory is small.

The hyperfine effect, which is very great in the $V-A$ theory for hydrogen capture,[17] disappears for He^3 capture in the limit of a pure $V-A$ theory at $q^2=0$ as can be seen from the following argument.[18] The trion doublet behaves similarly to the $\bar{n}$, $\bar{p}$ doublet, but under charge conjugation the $V-A$ theory becomes a $V+A$ theory for which the hyperfine effect is small. In the physical situation one expects a 30% difference in capture from the two hyperfine states of the He^3 mesonic atom, which in turn implies an 8% difference in the rates for capture from a statistical mixture and from the triplet ground state. Following the arguments of Telegdi and Winston,[19] there is no reasonable way by which the hyperfine population can change in times comparable to the muon lifetime. But even in the unlikely event that the capture is not from a statistical hyperfine mixture, the theoretical prediction is not grossly wrong.

Finally, muon capture in He^3 and in liquid hydrogen are complementary in that they measure different combinations of the coupling constants. Whereas the He^3 capture is from a statistical hyperfine ensemble, the initial state for the hydrogen capture is essentially $\frac{3}{4}$ singlet and $\frac{1}{4}$ triplet.[20]

The experimental plan and the apparatus are discussed in Sec. II. The several runs which were made and the data analysis are covered in Secs. III and IV, and Sec. V contains results and discussion.

II. EXPERIMENTAL TECHNIQUE

A. General

The bound triton in the reaction

$$\mu^-+He^3 \rightarrow H^3+\nu \tag{1}$$

is characterized by the discrete kinetic energy 1.897 MeV, whereas the reactions

$$\mu^-+He^3 \rightarrow d+n+\nu, \tag{2}$$

and

$$\mu^-+He^3 \rightarrow p+n+n+\nu \tag{3}$$

lead to a smoothly varying energy spectrum for the charged product extending to several MeV. The rate for reaction (2) +reaction (3) is expected to be about $\frac{1}{2}$ the rate for reaction (1),[16] and the muon decay rate from the ground state of the He^3 mesonic atom is ~ 300 times as great.

A high-pressure He^3-filled gas scintillation counter was used as the target for stopping muons. Reactions (1)–(3) yielded a composite energy-loss spectrum in the counter, delayed in time with respect to muon arrival. The triton count was readily extracted from this spectrum considering the following: (1) The thickness of the counter gas was the equivalent of 70 mg/cm^2 of He^3. Since the range of the recoil tritons is 2.3 mg/cm^2 of He^3 their full energy was observed with close to 100% efficiency. On the other hand, the decay electrons are minimum-ionizing and left no more than 0.3 MeV in the counter. They were cleanly separated from the tritons because of the good energy resolution of the counter. Furthermore, they were rejected with 90% efficiency by surrounding electron detectors. (2) Again, because of the good resolution, the triton peak stands out cleanly above the background from reactions (2) and (3). Therefore, the error due to background subtraction was kept small. (3) Muon capture to bound excited states of He^3 would appear as an enhancement of the triton peak but no such states have been observed.[21]

The triton formation rate λ_t was measured by comparison to the muon decay rate

$$\lambda_t=(t/e)\lambda_d. \tag{4}$$

t is the triton count, and e is the decay-electron count for muons stopped in He^3, each corrected for detection efficiency; λ_d is the muon decay rate in He^3.

[10] I. V. Falomkin *et al.*, Phys. Letters **3**, 229 (1963).
[11] L. B. Auerbach, R. J. Esterling, R. E. Hill, D. A. Jenkins, J. T. Lach, and N. H. Lipman, Phys. Rev. Letters **11**, 23 (1963); R. J. Esterling, thesis, University of California Radiation Laboratory Report UCRL 11004 (unpublished).
[12] C. Werntz, Nucl. Phys. **16**, 59 (1960).
[13] H. Collard *et al.*, Phys. Rev. Letters **11**, 132 (1963).
[14] L. I. Schiff, Phys. Rev. **133**, B802 (1964); J. S. Levinger, *ibid.* **131**, 2710 (1963); B. K. Srivastava, *ibid.* **133**, B545 (1964).
[15] A. Fujii and Y. Yamaguchi, Progr. Theoret. Phys. (Kyoto) **31**, 107 (1964).
[16] A. F. Yano, Phys. Rev. Letters **12**, 110 (1964); R. J. Oakes, Phys. Rev. **136**, B1848 (1964); W. Drechsler and B. Stech, Z. Physik **178**, 1 (1964); and A. Bietti, Phys. Letters (to be published).
[17] J. Bernstein, T. D. Lee, C. N. Yang, and H. Primakoff, Phys. Rev. **111**, 313 (1958).
[18] L. Wolfenstein (private communication).
[19] R. Winston, Phys. Rev. **129**, 2766 (1963); R. Winston and V. L. Telegdi, Phys. Rev. Letters **7**, 104 (1961).
[20] S. Weinberg, Phys. Rev. Letters **4**, 575 (1960).
[21] D. Strominger, J. M. Hollander, and G. T. Seaborg, Rev. Mod. Phys. **30**, 585 (1958): See Ref. 18G46.

The triton events were sorted in the two dimensions of pulse height and delay time with respect to the stopping muon. Simultaneously, decay electrons were time-sorted in the same apparatus so that in the analysis many systematic errors were avoided. These time analyses allowed random backgrounds to be subtracted out since events associated with the disappearance of the muon show the characteristic mean life of 2.19 μsec.

Several types of runs were made during the course of the experiment with different gas mixtures in the target counter. (1) Extensive preliminary studies were made of the experimental equipment with a mixture of 90% He^4 and 10% Xe (320 psi He and 40 psi Xe). (2) The efficiency of the electron detectors was measured in a run for which the mixture was nominally 50% He^4 and 50% Xe (200 psi Xe and 160 psi He). (3) A correction was made to the decay electron count for electrons from muons stopping in other low-Z material. This contamination was measured using 100% Xe in the counter. (4) The triton events were observed in the so-called "standard run" with the "standard mixture" of 90% He^3 and 10% Xe.

B. Gas Counter

1. Design. Noble-gas scintillants and the technology of their use have been discussed by several authors.[22,23] Our design relied to a great extent on this earlier work.

The gas counter consisted of three separate light-tight compartments in a cylindrical steel pressure vessel, as shown in Fig. 1. Counters 3 and 4 shared a common gas system of 100% Xe and were used both in the stopping muon telescope and in detecting decay electrons. The He counter, No. 5, was separated from counters 3 and 4 by a thin-walled (0.018 in.) cubical Ag box of one liter capacity. It was used in the stopping-muon telescope and to detect triton recoils. Counter 3 was viewed by one and counter 4 by three 6655A photomultiplier tubes through glass pressure windows. Counter 5 was viewed by a 5-in. phototube (EMI9579) through the glass window and light pipe on top of which was a $\frac{1}{16}$-in. thick CsI(Tl) crystal. The Ag box was coated inside and out with a diffusely reflecting layer of 10 mg/cm^2 of smoked CsI (pure)[24] and the remaining reflecting surfaces of the electron counter had a similar coating of MgO. Since scintillations for the gases used are primarily in the ultraviolet, all surfaces were coated with the wavelength shifter *p,p'*-diphenylstilbene, reflecting surfaces with 100 μg/cm^2 and transmitting surfaces with 25 μg/cm^2. The gases were maintained at 360 psi and 21°C during the experiment. In order not to rupture the Ag box the pressures of the two gas systems were maintained equal to within 0.1 psi at all times. The scintillation efficiency was stabilized by recirculating the gases through cold traps during the runs. For the first He^3 run this efficiency was reduced in counter 5 because of a trace of impurity not removed by the trap, so for the second run the He^3 was first purified in an activated charcoal trap before entering the counter.

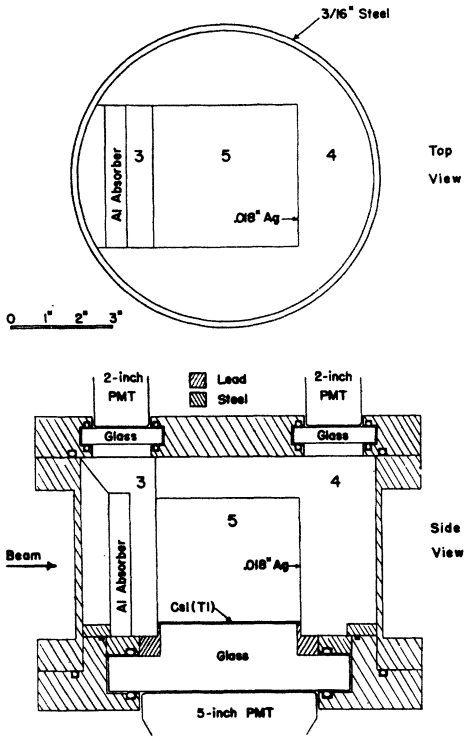

FIG. 1. Gas scintillation counters. Counters 3 and 4 were filled with pure Xe to a pressure of 360 psi. Counter 5 was filled to the same pressure with a mixture normally of 90% He-10% Xe. Counter walls were coated with 100 μg/cm^2 of diphenylstilbene (DPS) wavelength shifter upon a white diffuse surface. The top surface of the CsI(Tl) slab was coated with 25 μg/cm^2 of DPS. The space upstream from counter 3, while filled with xenon, was separated by a light-tight partition and contributed no scintillation light to counter 3. One of the three photomultiplier tubes which viewed counter 4 is shown.

It was of primary importance that the electron count not contain large contributions from muons stopping in elements other than He^3. To this end, as much as possible, the other materials in the immediate vicinity were of $Z \geq 47$ (Cs,I,Ag,Xe) for which the muon mean life $\tau < 0.1$ μsec.[25] The muon-induced activity in these elements was negligible by the time the count of delayed events was started 0.7 μsec after muon arrival. The low-Z wavelength shifter gave rise to a small measurable contamination. However, muons stopping in the glass could have been a source of a large number of electron counts. Such a muon was rejected by the following

[22] J. Northrup and R. Nobles, IRE Trans. Nucl. Sci. **3** (1956), and Nucleonics **14**, 36 (1956); R. Nobles, Rev. Sci. Instr. **27**, 280 (1956); J. Northrup, *ibid.* **29**, 437 (1958); J. Northrup and J. Gursky, Nucl. Instr. Methods **3**, 207 (1958); C. Huddleston, *Fast Neutron Physics* (Interscience Publishers, Inc., New York, 1961), Part I, Chap. III D; A. Sayres and C. S. Wu, Rev. Sci. Instr. **28**, 758 (1957).

[23] R. Shamu, Nucl. Instr. Methods **14**, 297 (1961).

[24] We are indebted to Dr. E. J. Sternglass for his advice on smoking CsI.

[25] T. A. Filippas, P. Palit, R. T. Siegel, and R. E. Welsh, Phys. Letters **6**, 118 (1963); J. C. Sens, Phys. Rev. **113**, 679 (1959).

scheme. From the geometry of the counter, if this muon gave a gas pulse it must also have passed through the CsI(Tl) crystal which has a characteristically long scintillation decay time of 0.55 μsec. A pulse-shape discrimination circuit (PSD) sorted out this long time component, and the muon was then prevented from triggering the counting system. PSD was also used to count decay electrons passing down out of counter 5.

The scintillation efficiency of He gas was increased by a factor of four with the admixture of 10% Xe.[22] Table I lists scintillation efficiencies for different fillings of the counter compared to the CsI(Tl). The source was the 5.3 MeV α of Po^{210}, always in place at the center of the counter. These tests indicate in addition to the changed scintillation efficiency an increasing scintillation decay time with increased Xe concentration.

Two questions may be raised about the admixing of Xe but neither turns out to be a problem. (1) Will all the muons capture atomically onto the Xe since it is much heavier than He? An estimate based on runs with two different Xe concentrations indicates somewhat fewer Xe atomic captures than predicted by the Fermi-Teller Z law. (2) Will the Xe steal muons from the He with a characteristic time comparable to or faster than the muon lifetime? In the case of muons stopping in liquid hydrogen, a trace impurity steals an inordinate number of muons from the neutral μ-p mesonic atom.[26] It was expected that the electron cloud was sufficient to prevent close proximity of the charged He^3-μ system and a Xe nucleus. In fact the μ^- lifetime in the gas mixture shows no indication of foreshortening due to stealing. Even if a small amount of such stealing did occur, the ratio t/e would not change. The Xe has the added important advantage of reducing the triton range by a factor of 2.5 so that the correction for escaping tritons was reduced.

2. Performance—target counter. The output of counter 5 was linear with respect to energy loss for particles of similar specific ionization as demonstrated in Fig. 2. The point at 0.76 MeV is for the thermal neutron reaction $n+He^3 \rightarrow H^3+p$ of cross section 5000 b. The points at 1.9 MeV and 5.3 MeV are for the recoil triton and the α source. The source was deposited on a needle whose diameter was comparable to the α range. Ultraviolet light hitting the needle was absorbed by it and thus the α point appears 10% lower than the line through the other points.

TABLE I. Response of target counter to α particles.

Scintillator	Pulse height[a] Current pulse	Charge pulse	Decay time[b] (nsec)
CsI(Tl)	1.0	1.0	1200
He	0.88	0.20	<30
Xe	2.20	0.83	90
HeXe (standard)	2.46	0.89	160

[a] Integration times at anode of phototube were 40 nsec for current pulse and 10 μsec for charge pulse.
[b] Decay time is defined as time for pulse height to change from 90 to 10% of maximum.

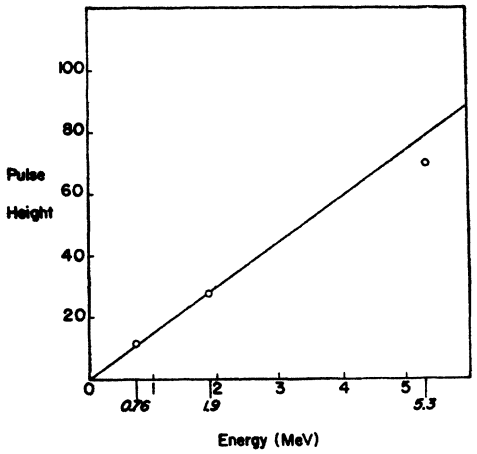

FIG. 2. Linearity of gas scintillation counter. The plotted point at 0.76 MeV corresponds to the charge-exchange reaction $He^3(n,p)H^3$; at 1.9 MeV to the recoil triton from muon capture; and at 5.3 MeV to Po^{210} α particles. The α particles did not give the full pulse height because of the shadow effect of the source needle.

The spatial uniformity of the counter was measured using a movable α source. This test gave a counter resolution due only to nonuniformity of 9.0% full width at half-maximum. For the first He^3 run the pulse-height spread was 26.6% for the triton peak and 35.6% for the neutron reaction (full width at half-maximum). For the second run with better scintillation efficiency, the widths were 15.0 and 18.3%. For either run the ratio of the two resolutions agrees with what one expects on the basis of photo-electron statistics and spatial uniformity.

There was no apparent change in scintillation efficiency during the course of either He^3 run. The ratio of pulse heights in gas and CsI(Tl) for the α source was the same at the beginning and the end of either run. An automatic gain stabilizing circuit operated on the α pulses to counteract any instability in the counter 5 system. The over-all response to the α source of counter and electronics was checked every eight hours. Variations from the mean were $<0.8\%$.

3. Performance—Xe counters. The primary energy calibration of counters 3 and 4 was based on beam electrons traversing either counter and the calculated energy loss in Xe.[27] Po^{210} α sources in these counters were used as secondary standards only. The shadow effect of the α-source holder was so great in this dense gas as to make for a 15% uncertainty in the energy associated with the peak in the pulse height spectrum. In addition

[26] E. Bleser, E. W. Anderson, L. M. Lederman, S. L. Meyer, J. L. Rosen, J. E. Rothberg, and I-T. Wang, Phys. Rev. 132, 2679 (1963).

[27] R. Sternheimer, in *Methods of Experimental Physics*, edited by L. C. L. Yuan and C. S. Wu (Academic Press Inc., New York, 1961), Vol. 5, Part A, Chap. 1.1, p. 1; and Phys. Rev. **103**, 511 (1956).

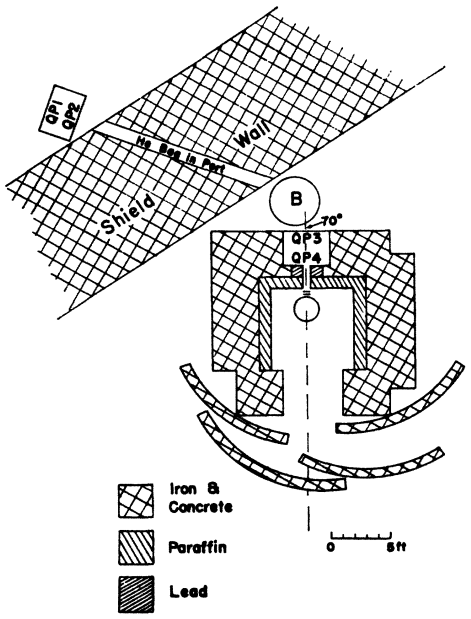

FIG. 3. Floor plan of experimental area showing beam magnets and the paraffin-lined blockhouse. The bending angle of magnet B was 70° for beam particles of the selected momentum.

there is a striking dependence of scintillation efficiency on specific ionization. Shamu[23] has observed that in Xe minimum-ionizing particles give rise to a *lower* scintillation response than α particles by a factor of 1.6. Our observations agree with this.

There was a sizeable spread in pulse height in these counters for decay electrons. First, the energy loss was not unique due to the variable path length traversed, and second, the light collection efficiency was not uniform for these odd shapes. There are additional contributions to this spread from the Landau effect and from photoelectron statistics. Based on the spectra of beam electrons the overall resolutions were 90% for counter 3 and 60% for counter 4 (full width at half-maximum). These widths are large but but are sufficient to the purpose, since the integrated count is what is required.

The Xe counters were stable. There was no significant change in scintillation response over the course of the experiment.

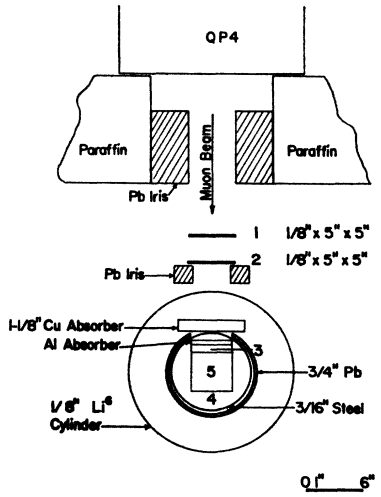

FIG. 4. Disposition of counters and beam-restricting lead irises. The Li^6 cylinder is closed above by a Li^6 sheet and below by a boral sheet.

C. Floor Layout and Beam

The experimental layout is shown in Fig. 3. The meson beam was bent 70° upon leaving the shielding wall hole and was intensified by a factor of 2 by quadrupole magnets and He bags. The beam then entered a shielding house of steel, concrete, and lead with a 1-foot thick lining of paraffin to thermalize neutrons. The counters and all the gas-handling equipment were inside this house. Figure 4 shows more detail of the counter setup. Immediately around the gas counter was $\frac{3}{4}$ in. of Pb for shielding against low-energy γ rays, and around the whole gas counter assembly there was a $\frac{1}{8}$-in.-thick cylinder of Li^6 for shielding against slow neutrons.[28]

Random γ-ray background was of particular concern in the decay electron count. There was approximately one kg of Xe in counters 3 and 4 so they made efficient low-energy γ detectors. In Sec. IIIA it will be shown that this background was held to better than a manageable level. Thermal neutrons were a problem because of the $He^3(n,p)H^3$ reaction mentioned earlier. Had there been more of these events than there were, they could have masked a portion of the recoil-triton peak.

Counters 1 and 2 were standard plastic scintillators $5\times5\times\frac{1}{8}$ in. The beam was collimated to 4×4 in. by the final Pb iris and slowed down by the Cu and Al absorbers.

The meson beam was stretched to a duty factor of 2 by the internal rotating target and the bending magnet selected a particle momentum of 166 MeV/c. Figure 5 shows the differential range curve for this beam taken with the gas counter. A compromise was made between muon intensity and freedom from pion and electron contamination. Since the triton count is normalized to decay electrons and not to the beam count the only reason for having a purer muon beam would be the lower random background it would afford. The range increments corresponding to the three gas mixtures used in the target counter are shown in Fig. 5. Since the comparison of these runs is based to some extent on the similarity of the stopped muon distributions in the counter, it is important to note that the muon intensity is essentially constant over any of the increments. During the triton count the average rate for muons stopping in He^3 was 3.5 sec^{-1}.

D. Electronics

In general the electronics for this experiment were transistorized. A block diagram is shown in Fig. 6.

[28] The Li^6 was rented from Oak Ridge National Laboratory.

Pulses from the five counters were distributed, amplified as required, and sent to one of essentially three places: (1) fast-coincidence circuits for beam telescopes, (2) pulse-shape and pulse-height discriminators, the outputs of which were used both to refine the definition of beam counts and for delayed event coincidences, and (3) the linear system for pulse-height analysis.

Before distribution the pulse from counter 5 was stabilized in a circuit based on the one of Marlow.[29] That is, the gain of the circuit was automatically adjusted to maintain α-source pulses at a fixed voltage level. The stability factor for this circuit was 100 so there was no significant drift in the No. 5 pulse sent to the rest of the electronics.

1. Beam monitors. The following fast coincidences (10-nsec resolving time) were made in transistorized cir-

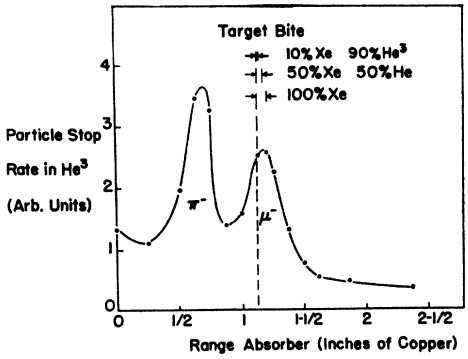

FIG. 5. Differential-range curve of negative-muon beam. The target bite of each of the gas mixtures in counter 5 is shown in equivalent thicknesses of copper. Fe and other material in the beam are not included in absorber thickness.

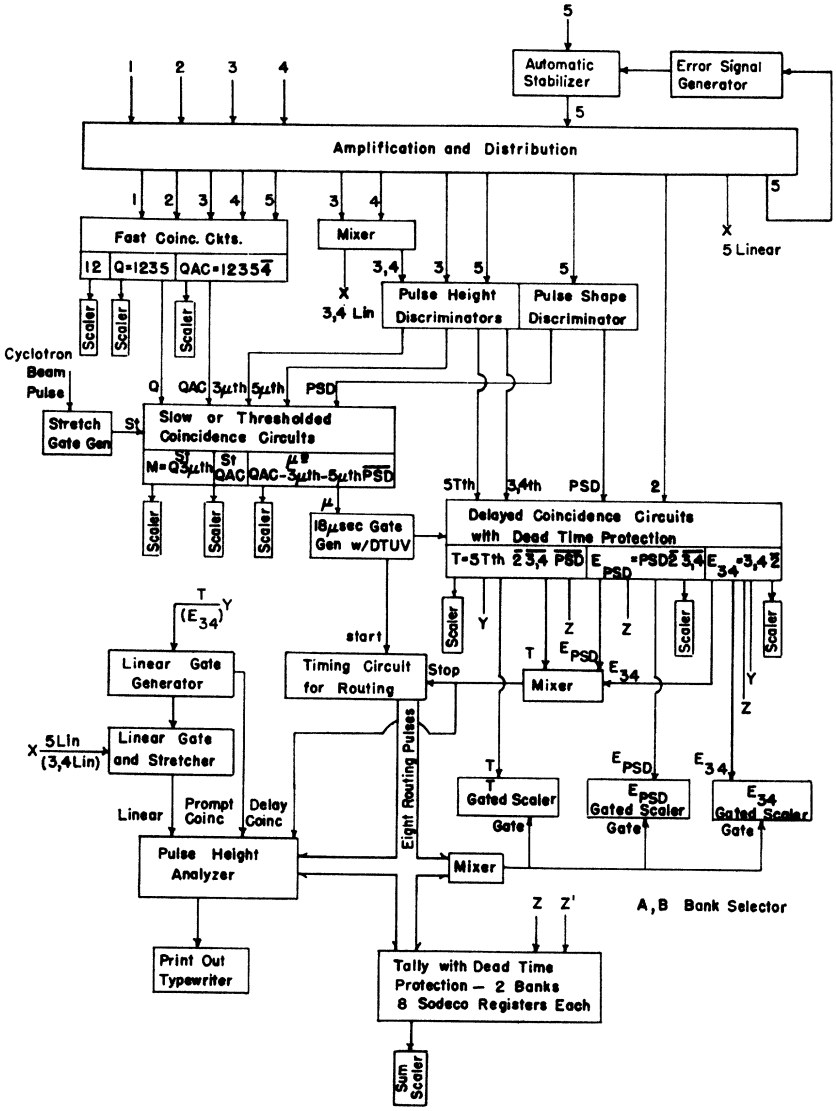

FIG. 6. Block diagram of electronics. The block marked "Amplification and Distribution" indicates the appropriate Hewlett-Packard or transistorized amplifiers. Individual emitter followers for each output provided the distribution. The "μ" coincidence was formed in the block "slow or thresholded coincidence circuit." The "timing circuit" had eight output cables for producing coincidences with delayed events in the appropriate time bins of either the PHA or Sodeco register banks.

[29] K. Marlow, Nucl. Instr. Methods 15, 188 (1962).

cuits of the Garwin type: $Q \equiv 1235$ (any particle which passed through counters 1, 2, and 3, and entered No. 5); and $QAC = 1235\bar{4}$ (a particle which entered No. 5 but did not enter No. 4). The thresholds for the gas-counter pulses in these coincidences were set very low.

The stopped-muon coincidence, μ, was derived from QAC with additional coincidence conditions which tended to select against muons stopping in material other than He. A muon which stopped in counter 5 usually gave up a large amount of energy in it; a muon which penetrated the counter walls or the glass was less heavily ionizing in the gas and therefore left less energy the farther it penetrated. Many of these penetrating muons were rejected by requiring a high threshold for the No. 5 pulse in the "5μth" discriminator. The discriminator "3μth" on the muon pulse in counter 3 served a similar purpose. These thresholds had the added feature of rejecting most beam electrons. A pulse shape discriminator pulse, PSD, indicated a long-time component in the No. 5 pulse from the CsI(Tl) crystal regardless of any short-time component from the gas. The circuit was based on one by Forté.[30] It was highly efficient in rejecting muons which penetrated the CsI(Tl) crystal because these particles were densely ionizing. It was also demonstrated to be highly efficient in counting the lightly ionizing decay electrons and this added confidence in its ability to reject muons stopping in the glass. Finally, it was required that the stopped muon occur in the stretched part of the beam to minimize random background. All told then, a stopping muon was defined as

$$\mu \equiv \mathrm{St}QAC - 5\mu\mathrm{th} - 3\mu\mathrm{th} - \bar{\mathrm{P}}\bar{\mathrm{S}}\bar{\mathrm{D}}.$$

Since pions stopped mostly upstream of counter 5 and electrons were mostly rejected by the threshold conditions, the "μ" counts were almost entirely from muons. There was a large contribution to μ from stops in the Ag walls and in the Xe of counter 5 so that of the μ rate of 25 sec^{-1}, 1/7 were stops in the He^3.

The coincidence M was defined as

$$M \equiv \mathrm{St}Q - 3\mu\mathrm{th}.$$

It was a count of all muons entering counter 5, and was required for a comparison of the "pure Xe" run to the primary-decay-electron count.

Additional monitor counts were taken, as indicated in the drawing, for consistency checks.

2. Delayed events. A delayed event was one of three possible types: A recoil triton, a decay electron counted in either Xe counter, or a decay electron counted by PSD. All the inputs to these circuits were shaped pulses from the pulse-height discriminators and the PSD circuit. These types are defined as

triton candidate: 5 ($\bar{3}$ or $\bar{4}$) $\bar{\mathrm{P}}\bar{\mathrm{S}}\bar{\mathrm{D}}$ $\bar{2}$
electron in Xe: (3 or 4) $\bar{2}$
electron in CsI(Tl): PSD ($\bar{3}$ or $\bar{4}$) $\bar{2}$

where the bars indicate anticoincidence. For example, a triton candidate was a count in 5 only—it was not a decay electron or cosmic ray which registered in any of the surrounding counters; nor was it coincident with a beam particle. The thresholds for the pulse-height discriminators were checked every eight hours and found to vary by not more than 2.5%. The PSD was checked less frequently, and found to be very stable. The stability for the delayed event thresholds was crucial to a constant electron detection efficiency.

The μ pulse triggered an 18.3-μsec gate through which delayed events passed if they came between 0.7 and 19.0 μsec after muon arrival. It was essential to the system that no more than one event per gate be accepted. To this end a dead time prevented any delayed event coincidence if there had been one during the previous 25 μsec. This arrangement also prevented time skewing of random background. That is, any amount of random background did not alter the time constant in the muon lifetime curve. The gated counts are labeled T, E_{34}, and E_{PSD}.[31]

3. Timing system. The timing circuit sorted the delayed event pulse into one of eight time bins. Nominally the first four bins were each 1.0 μsec long, the next three were 2.0 μsec long and the eighth was 7.7 μsec long in order to accumulate good statistics on the random background. The spacing and widths of the time bins were determined by delay cable for stability. The system was started by the μ pulse and stopped by the mixed gated delayed events. From the timing system the eight "routing pulses" went both to the pulse-height analyzer for two-dimensional analysis and to the two banks of Sodeco registers. At this point the routing pulse represented any of the three types of delayed events. It was decoded in the pulse-height analyzer by the prompt coincidence condition and in the register system by suitable "enable" pulses. Since the registers were slow there was dead-time protection in the register system, and the dead-time factor was measured with more than adequate precision. During the standard run, triton events were stored in the pulse-height analyzer and the two types of electron events in the two sets of registers.

It must be emphasized that since the ratio t/e was measured, the final result is insensitive to small errors in calibration of the timing system. In addition, since the t and e counts were taken simultaneously, effects like varying dead time in the system due to beam rate fluctuations did not affect the ratio. In fact, the system was shown capable of measuring correct mean lives, a more sensitive test than the measurement of a time-integrated count.

The circuit was calibrated four times during the experiment with a Tektronix oscilloscope delay pulse generator, which was itself calibrated with a precision crystal oscillator. In addition, the system was tested in

[30] M. Forté, Nuovo Cimento Suppl. 9, 390 (1958).

[31] At times when counter 3 or 4 was studied separately the (3 or 4) condition was changed appropriately to give E_3 or E_4.

several other ways: (1) Analysis of random pulses measured the relative widths of channels to 1%. (2) Measurement of the μ^+ lifetime yielded $\tau=2.208 \times(1\pm0.005)$ μsec. (3) Measurement of the μ^- lifetime in He^4 (with 10% Xe present) yielded $\tau=2.203$ (1 ± 0.005) μsec when corrected for nuclear capture.[32,11] The errors in the measurements are primarily due to the uncertainty in calibration. The μ^+ lifetime is in good agreement with the accepted value of 2.200 ± 0.001 μsec.[33] But more important, the agreement for μ^+ and μ^- demonstrates that (1) there was no significant stealing of muons by Xe, (2) any contribution to the count from muons in heavy elements was negligible, and (3) with high confidence there was $<7\%$ contamination due to muons stopping in glass. The "pure Xe" run measured the last more precisely.

4. Linear system. During a standard data run the delayed pulse from No. 5 was analyzed in the RIDL 400-channel pulse-height analyzer. The linear pulse was first put through the fast linear gate (width 0.3 μsec) and then stretched to match the analyzer. The T pulse triggered the gate. A fast gate was required to prevent the pulses from the stopped muon and the delayed event from mixing in the slow amplifier of the analyzer. The analyzer was divided into eight subgroups of 50 pulse-height channels each, each subgroup associated with one of the eight time bins. The routing pulse from the timing system directed the linear pulse to the proper subgroup. The complete system was checked with a pulser and found to be quite linear in the region of interest.

III. DECAY-ELECTRON COUNT

A. Electron Analysis

A two-dimensional analysis was made of the response of each of the Xe counters to decay electrons from the standard target gas mixture. Figure 7 shows typical pulse-height spectra for these counters with random background subtracted out. For counter 3 there were a large number of counts at small pulse heights due to afterpulses[34] from the stopping-muon pulse. Therefore, in taking the integrated electron count during a standard run the counter-3 threshold for delayed events was set high enough so that afterpulses were a small contamination (later accounted for). This high threshold necessarily meant that the counter 3 efficiency was reduced to

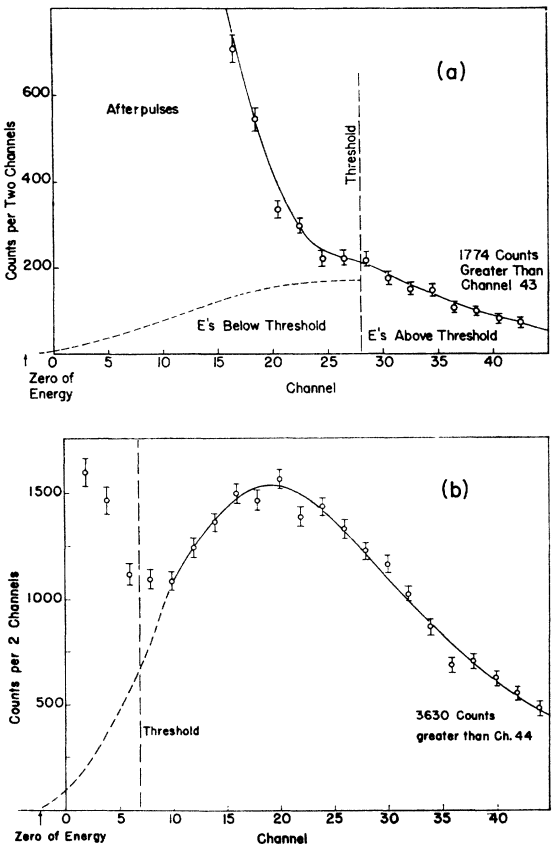

FIG. 7. Pulse-height distribution for decay electrons detected in counters 3 and 4 with random background subtracted. The dashed portion of the curve represents an estimate of the true shape of the spectrum. The target gas was the standard mixture.

60% of geometrical. The counter-4 spectrum is of the expected shape except for the excess of low-energy counts, the origin of which was not certain. The dashed line shows an estimate of the correct shape of the curve in the low-energy region. With the threshold set as shown, the efficiency was 96% of geometrical.

Time analyses were performed by fitting the data to the curve

$$dN/dt=A\lambda e^{-\lambda t}+B, \tag{5}$$

where A is the time-integrated count of muon-associated events. The Appendix discusses a refined form which in the case of the decay electron count leads to a 0.2% change in A. Two methods of fitting the curve were used: (1) A least-squares fit was made varying A, λ, and B. This approach was used when checking the timing system and to detect the presence of contamination either from afterpulses or muons stopping in material other than He. The curves in Fig. 8 show the time spectra respectively for E_{34}, E_4, and E_{PSD} during the first He^3 filling. The experimental points are the properly normalized counts with random background removed. The solid lines are visual fits to the data of a simple exponential with mean life 2.19 μsec. In curve 8a the

[32] R. Bizzarri, E. Di Capua, U. Dore, G. C. Gialanella, P. Guidoni, and I. Laakso, Phys. Letters 3, 151 (1962); *ibid.* 3, 312 (E) (1962). M. M. Block *et al.*, Brookhaven National Laboratory Report BNL 837 (C-39) 1963 (unpublished), p. 309.

[33] R. Lundy, Phys. Rev. **125**, 1686 (1962); M. Eckhause, T. Filippas, R. Sutton and R. Welsh, *ibid.* **132**, 422 (1963); S. Meyer *et al.*, *ibid.* **132**, 2693 (1963); F. J. M. Farley, T. Massam, T. Muller, and A. Zichichi, in *Proceedings of the 1962 Annual International Conference on High-Energy Physics at CERN* (CERN Scientific Information Service, Geneva, Switzerland, 1962), p. 415.

[34] The term "afterpulse" is used to include possible contributions from afterglow in the scintillant as well as pulses generated in the phototubes by positive ions formed in the residual gas.

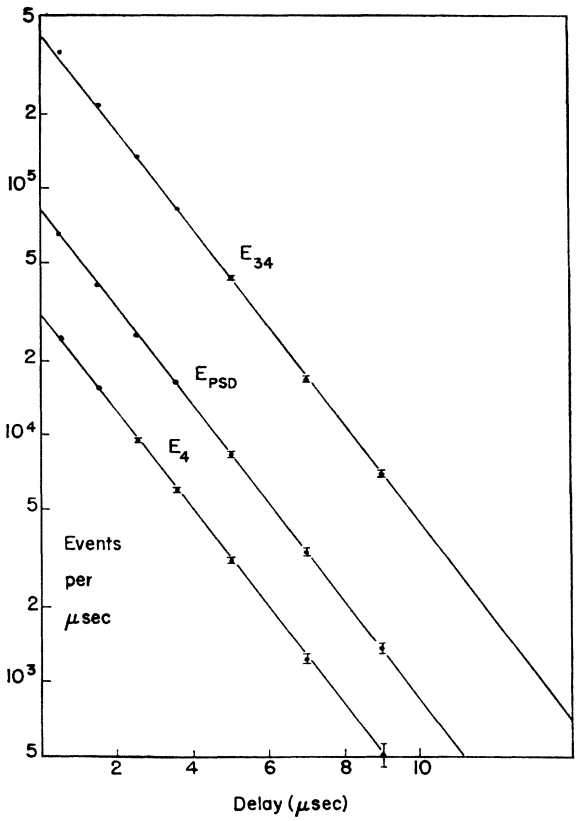

FIG. 8. Time spectra for the decay-electron data of the first "standard" run. The data points are suitably normalized and random background has been subtracted. The solid lines are visual fits for a mean life of 2.19 μsec. In each case the background rate is <2% of the decay rate in the first time bin. E_{34}: Afterpulses cause a barely-visible deviation from the line in the first four time groups. These deviations (in units of standard deviations) are 41.2, 12.4, 10.4, and 4.6 for the time groups I, II, III, and IV, respectively. A least-squares fit to all data including afterpulses gave a mean life of 2.130±0.034 μsec (statistical error only). The χ^2 was 181, where 5 was expected from a simple time dependence. E_4: A least-squares fit to all points determined a mean life of 2.178±0.011 μsec (statistical error only) with a χ^2 of 4.2, where 5 was expected. E_{PSD}: A least-squares fit determined a mean life of 2.205±0.007 μsec (statistical error only) and a χ^2 of 6.2 where 5 was expected.

afterpulse contamination of counter 3 is apparent. The fitted mean life is 2.130±0.0034 μsec with a χ^2 of 181 instead of the expected 5. The mean life and χ^2 for E_4 and E_{PSD} are, respectively,

$$\tau_4=2.178\pm0.011\ \mu\text{sec},\quad \chi^2=4.2,$$
$$\tau_{PSD}=2.205\pm0.007\ \mu\text{sec},\quad \chi^2=6.2,$$

which demonstrate the cleanliness of these data. The quoted errors are statistical only. (2) In the "time window method," λ was assumed to be $0.4566\times10^6\ \text{sec}^{-1}$. Two time channels were constructed of time groups 1-6 and 7-8, respectively. The amplitudes A and B and their errors were derived from these two numbers. This approach was used for the triton count because of the small number of counts in a given pulse-height channel. To be consistent, it was always used to extract amplitudes of curves. Note that a 1% change in the assumed value of λ leads to a change in A of 0.08%.

B. Electron Counting Efficiency—Measurement

It was the intention in the design of this experiment that the electron detection efficiency be close to 100% (see Fig. 1.). The E_{PSD} by itself was demonstrated to be well plateaued in efficiency during the first He^3 run by varying its threshold, but because of the nonzero thresholds for counters 3 and 4 the overall efficiency was 87%.

1. Efficiency tests. The efficiency for detection in counters 3 and 4, η_3 and η_4, were measured in an auxiliary run for which the gas mixture in counter 5 was 50% He^4 and 50% Xe. With the added stopping power, more than 90% of decay electrons could be counted in No. 5 above tube noise, afterpulses, and low-energy background.[35] The efficiency of counter 4, for example, was the ratio of electrons detected simultaneously in counters 5 and 4 to the total number detected in counter 5. It therefore includes both geometrical and pulse-threshold effects. Since the detection efficiency of No. 5 cancels in this ratio it need not be known precisely. In the notation of this experiment

$$\eta_4=\frac{E_4'}{E_4'+T+E_{PSD}}\quad\text{and}\quad\eta_3=\frac{E_3'}{E_3'+T+E_{PSD}},\qquad(6)$$

where $E_4'=54\bar{2}$, $E_3'=53\bar{2}$ and a random background subtraction has been made from all counts. Efficiencies were measured for two delayed event thresholds in counter 5 corresponding to electron path lengths in that counter of 2 and 4 cm, respectively. For the lower threshold $\eta_4=0.627$, and for the higher threshold $\eta_4=0.618$. One may expect that η_4 was sensitive to the stopped muon distribution but this tends not to be so because of the low-electronic threshold in No. 4 and because No. 4 covers $\frac{2}{3}$ of the He counter.

The electron detection efficiency of counter 5 for the 50-50 gas mixture was measured with sufficient precision by comparing the E_4' count rate to a measurement of that rate with the No. 5 requirement removed; i.e., E_4'/E_4. This efficiency was 88 and 57% for the 2- and 4-cm thresholds, respectively. Because of the good agreement for markedly different counting rates, the final value of η_4 was taken as the weighted mean of the two measurements. Twelve percent of the muons were not sampled by the count at the 2-cm threshold. The error includes a 1% uncertainty for the contribution to η_4 from these muons. Thus $\eta_4=0.625\ (1\pm0.024)$.

Similar measurements of η_3 gave 0.102 and 0.116 for the 2- and 4-cm thresholds in counter 5. These numbers

[35] Afterpulses in counter 5 were bunched at early times with no noticeable effect after 3.0 μsec after muon arrival. Therefore, all efficiency runs were taken with the start of the muon gate advanced to 3.5 μsec. It should be noted that the size of an afterpulse was the equivalent of ≤0.3 MeV so these pulses were never confused with tritons in the standard run.

contain no afterpulse contamination from counter 3 because of the added No. 5 requirements in the definition of $E_3 \cdot \eta_3$ is more sensitive to the stopped muon distribution because of the high counter 3 threshold and because it covers only one face of counter 5. Thus: $\eta_3 = 0.116\ (1 \pm 0.055)$.

It is important to assure that the electron efficiency of counter 4 with the standard mixture in counter 5 is the same as the value of η_4 measured in the efficiency run. A shift in the stopped-muon distribution could have caused such a change. The Monte Carlo calculation (see Sec. IIIC) showed that the change in η_4 in going from the "50-50" to the standard gas mixture was $(-0.6 \pm 0.4)\%$, while for η_3 the change was 4.3%. A correction in agreement with these is also obtained by comparing the ratio η_3/η_4 taken from the efficiency test to the ratio $(E_3/\text{normalizer})/(E_4/\text{normalizer})$ measured with the standard mixture. The two ratios are $0.182(1 \pm 0.05)$ and $0.188(1 \pm 0.07)$, respectively. Considering the geometry of the counters this difference in the ratios is reflected in a change in η_4 of $(-0.7 \pm 1.7)\%$. Although the calculated effect is more precise than the measured one, the error in the latter is the assumed one. The corrected efficiencies are

$$\eta_4 = 0.621(1 \pm 0.029) \quad \text{and} \quad \eta_3 = 0.121(1 \pm 0.06). \quad (7)$$

The loss of electrons due to range absorption and bremsstrahlung in the target counter was $<0.1\%$ for the standard and "50-50" gas mixtures.

2. η_{34} and η_{PSD}. η_{34} is the efficiency of counters 3 and 4 treated as a unit, and η_{PSD} is the efficiency of the CsI(Tl) system, where again both geometrical and threshold effects are included. Neither η_{34} nor η_{PSD} could be measured in the same manner as η_3 and η_4. Because of the counter overlap $\eta_{34} < \eta_3 + \eta_4$. Further, during the standard run some afterpulses in counter 3 were included in E_{34} wheras there are none in η_3. The technique could not be used for η_{PSD} because of the altered significance of the counter 5 threshold when both gas and CsI light contribute to a pulse. Therefore these efficiences were measured by comparison to η_4 and with the standard gas mixture in counter 5.

$$\eta_{34} = \eta_4 \left(\frac{E_{34}/\text{normalizer}}{E_4\ /\text{normalizer}} \right),$$

where E_{34} and E_4 were measured in successive runs.

Similarily, $\eta_{PSD} = \eta_4(E_{PSD}/E_4)$, where the counts are taken in the same run. Thus,

$$\begin{aligned} \eta_{34} &= 0.748(1 \pm 0.033), \\ \eta_{PSD} &= 0.153(1 \pm 0.034). \end{aligned} \quad (8)$$

Since afterpulses constituted 21% of the E_3 count they were 3.5% of the E_{34} count. This contamination was constant throughout the run since for the eight-hour runs the rms deviation of E_{34}/E_{PSD} was 1.4%. Therefore, since all electron counts were compared to η_4, the final count is independent of the presence of afterpulses.

The sensitivity of η_3 and η_4 to the delayed event thresholds for counters 3 and 4 was evaluated from the pulse-height spectra taken during the efficiency tests. A 2% change in threshold yields a change in η_4 of 0.5%. A negligible error is introduced into η by taking an over-all efficiency based on the average thresholds for counters 3 and 4. Also note that though the afterpulses in No. 3 were an annoying problem we are confident that the total electron count based on E_{34} is correct. The electron count based on E_{PSD} has no afterpulse problem yet the two calculations agree to within 1%.

C. Electron Counting Efficiency—Calculation

A Monte Carlo calculation was made of the stopped-muon distribution from which the following were then derived: (1) the geometrical detection efficiencies of the three electron detectors, (2) the small difference between the detection efficiencies for the "50-50" gas mixture and the standard mixture, and (3) the correction to the triton count for those escaping the He counter.

The calculation was done in the following way. The differential probability that the muons enter the counter at angles θ, ϕ with respect to the normal to the front wall is

$$dP = N \exp[-\tfrac{1}{2}(\theta/\bar{\theta})^2] d\Omega dR, \quad (9)$$

where R is residual range in the counter, Ω is solid angle, $\bar{\theta}$ is the root-mean-square scattering angle, and N is a normalizing constant. It was assumed that all residual ranges R which met the threshold condition and all azimuthal angles ϕ were equally probable, but that $\bar{\theta}$ was a function of R as well as of the material upstream of counter 5. For example, those muons which barely met the threshold condition entered the counter essentially isotropically, i.e., $\bar{\theta} \gg 1$ rad, while for those that stopped at the downstream wall $\bar{\theta} = 0.8$ rad upon entering the counter. The calculation was also made for $\bar{\theta}$ independent of R with these two extreme values as an aid in fixing errors. The scintillation efficiency for a stopping muon is intermediate between the efficiencies for α particles and electrons. Therefore, at threshold, 4.0 mm $< R <$ 9.0 mm. The calculation was made for the two extreme cases. Two extreme cases were used of illumination density over the front face of the counter: (1) uniform illumination, and (2) all muons entering at the center of the front face. In fact, the illumination density at the front face is a smoothly varying function peaked at the center. Calculations were made corresponding both to the standard and "50-50" gas mixtures. An auxiliary result of the calculation is a pulse-height spectrum for the stopping muons which was measured in a run with the standard gas mixture. The measured spectrum agrees well with the calculated one.

The geometrical efficiencies for the three electron detectors were 0.204, 0.626, and 0.155 for E_3, E_4, and

E_{PSD}, respectively, for the standard mixture. Correction factors for the threshold requirements are 0.60, 0.96, and 0.99, respectively (see Fig. 7). Finally, the calculated efficiencies are $\eta_3=0.122$, $\eta_4=0.601$, and $\eta_{PSD}=0.154$. These are in very good agreement with the measured values [see Eqs. (7) and (8)], although the uncertainties are greater. They are presented as corroborative evidence though they do not enter into the final evaluation of the electron count.

D. "Pure Xe" Test

A count of decay electrons from low-Z material other than He was taken with 100% Xe in counter 5. The count was normalized to the monitor M which measured muons entering No. 5 but was independent of the mass of the counter gas. From a comparison to the He^3 runs the contamination in the electron counts was $(2.1\pm0.7)\%$.

An estimate can be made of the fraction of muons stopping in the wavelength shifter as compared to stops in He. Taking account of the nonuniform muon stop distribution this ratio is 1.8%. Thus, virtually none of the electron contamination was from muons stopping in glass.

E. Final Electron Count

The final electron counts for the two standard runs are shown in Table II. Listed are the total number of electrons counted and the corrected values. For the first run either the E_{PSD} count or the E_{34} count could be used. The average of the two is the quoted result. In the second run, because of the increased scintillation efficiency, it was necessary to run with a reduced η_{PSD}. Therefore, only the one calculation of E based on E_{34} could be made. However, by comparison to the "pure Xe" test for which η_{PSD} was also reduced it is assured that the PSD circuit was still fully sensitive to muons penetrating the CsI crystal. The errors quoted include all the known contributions. These are listed in Table III.

IV. TRITON COUNT

The triton count for the two runs was derived from the two-dimensional sort of the T pulses. Each pulse-height channel was time-analyzed using the time-window method to remove random background. The remaining time-dependent background under the triton peak was removed by a curve-fitting process, and the correction for escaping tritons was made on the basis of the Monte Carlo calculation of the stopped muon distribution.

TABLE II. Electron counts.

Run	η_{34}	η_{PSD}	Raw count E_{34}	Raw count E_{PSD}	Corrected count
T_1	0.748	0.152	8.576×10^5	1.728×10^5	1.592×10^6
					1.578×10^6
T_1(av)					$1.585\times10^6\times(1\pm0.033)$
T_2	0.748		4.822×10^5		$8.49\times10^5\times(1\pm0.035)$

A. Triton Spectra

The triton pulse-height spectra for the two runs, T_1 and T_2, are presented in Fig. 9 with random background subtracted. For both runs, but especially for the second one, with the fully purified gas, the triton peak stands out cleanly above the rather flat time-dependent background and is well separated from the large number of counts at lower energies. For either run, the triton peak is consistent with a Gaussian shape. The resolutions for the two peaks were 26.6 and 15.0% full width at half-maximum, respectively. It is expected that the time-dependent background for energies above 1.0 MeV is due to muon capture to the unbound states of H^3 (reactions 2 and 3). The contamination in this background from muon capture in other light elements should not be more than 15%. The counts below 1.0 MeV have two components: (1) Decay electrons which escape detection in the Xe counter were still 30 times more numerous than tritons. The peak for their energy spectrum was well below the electronic threshold for T pulses, but there is a tail which extends to $\sim$0.8 MeV. (2) Also, there is a residual peak in the time-dependent curve near channel 10 from the $He^3(n,p)H^3$ reaction. The residual effect is 6% of the raw count in the neutron peak. There were two instrumental effects which could give rise to it. (a) Pulse heights in 5 were shifted at early times due to base line shift in the linear system following a large stopped-muon pulse. The time-dependent spectrum was corrected for this effect by shifting the spectrum for each time bin appropriately, but because of varying base lines within a given time bin, the correction could not be exact. (b) The random background contributed to the time-dependent counts

TABLE III. Errors in electron counts.

Run	Source of error	Error (%)
T_1	η_{34} and η_{PSD} combined[a]	3.2
	"Pure Xe" test[b]	0.7
	Timing-circuit calibration[b,c]	0.5
	Electron threshold	0.2
	Statistics in electron count[d]	0.5
	Over-all[e]	3.3
T_2	η_{34}[a,b]	3.3
	"Pure Xe" test[b]	0.7
	Timing-circuit calibration[b,c]	0.5
	Electron threshold	0.3
	Statistics in electron count[d]	0.6
	Over-all[e]	3.5

[a] Error in η_{34} common to both runs.
[b] Error common to both runs.
[c] Error common to t and e counts and drops out of the ratio t/e. It also cancels in ratios taken in efficiency measurements.
[d] Includes uncertainty in random-background subtraction.
[e] Note that by and large, errors are common to the two runs.

because a background pulse would not be processed if it was preceded by a muon-associated delayed event (see Appendix). This effect accounted for 40% of the neutron residue which remained after the "base line shift correction." Both these corrections have been made in computing the data points. Most probably the remaining "neutron" counts are due to the incomplete "base line shift correction." The triton count was not affected by either of these considerations.

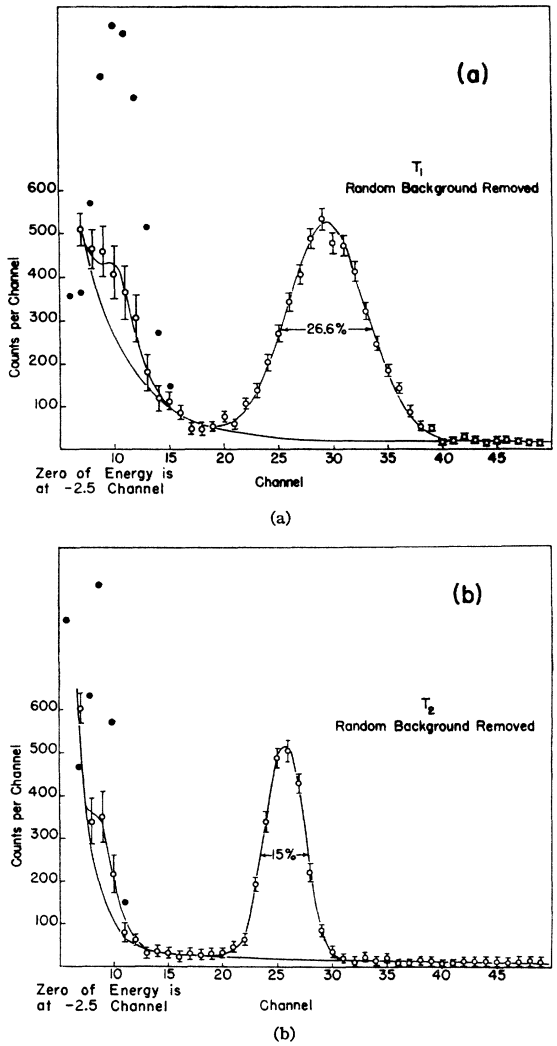

FIG. 9. Recoil-triton data. (a) T_1: count with random background subtracted. (b) T_2: count with random background subtracted. The curves represent fitted time-dependent background and the sum of this background and Gaussian fits to the triton and residual neutron peaks. The solid circles are for the reaction $He^3(n,p)H^3$, $Q=0.76$. They represent counts at early times after muon arrival before the random background subtraction. These are included for the purpose of energy calibration but are not on the same ordinate scale.

A time plot of the counts in the region of the triton peak shows a mean life consistent with the one measured for decay electrons. Figure 10 is the fit to the T_1 data

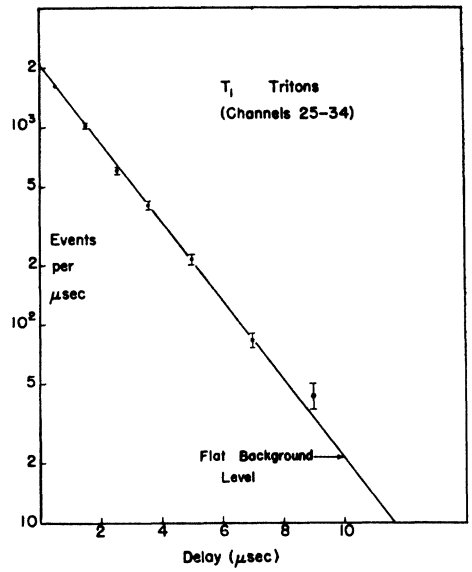

FIG. 10. Time spectrum of tritons in T_1 data. Flat background has been removed. The line shown is an exponential with a mean life of 2.19 μsec. A least-squares fit to all points determined a mean life of 2.25±0.05 μsec, and a χ^2 of 5.1, where 5 was expected. A similar analysis for T_2 gave a mean life of $\tau=2.18\pm0.07$ with a χ^2 of 2.4.

for pulse-height channels 25 to 34. A similar fit was made to the T_2 data for channels 19 to 32. For T_1 the fitted mean life is 2.25±0.05 μsec with a χ^2 of 5.1 where 5 was expected. For T_2 the mean life was 2.18±0.07 μsec with $\chi^2=2.4$. Therefore, the peak at 1.9 MeV has the right energy to fit reaction (1), and, in addition, it must be associated with a stopping muon.

B. Analysis of Time-Dependent Background

The size of the smoothly varying time-dependent background under the triton peak was evaluated on the basis of a least-squares fit to the points above 1.0 MeV. For the T_2 data two approaches were used: (1) A simple mathematical form was assumed for the background and a fit made to the points below and above the triton peak (pulse-height channels 13–18 and 33–49). The fitted background form was evaluated in the triton region and subtracted from the total count to give the triton count. The five different forms used and the resulting triton counts are listed in Table IV. (2) With a Gaussian form for the peak and one of the five forms for the background, all the points above 1.0 MeV were fit (channels 13–49). Approach 2 gave a mean triton count which was 1% lower than the mean count from approach 1. However, for T_2, counter uniformity was an important contribution to the spectral resolution, so the assumption of the Gaussian form may not have been entirely justified. Therefore the final triton count for T_2 is based on approach 1. The background subtraction was nearly independent of the form used. An assigned uncertainty of ±1.4% in the triton count due

TABLE IV. Triton count with time-dependent background subtraction.

Run	Background curve form	χ^2[a]	Tritons	$R=\frac{\text{background count}^b}{\text{triton event}}$
T_2[c]	A_1x+A_2	26	2520	0.179
	$A_1x^2+A_2x+A_3$	20	2528	0.173
	$A_1/x+A_2$	21	2532	0.170
	$A_1/x^2+A_2/x+A_3$	19	2577	0.149
	$A_1\exp(-A_2x)+A_3$	19	2552	0.162
	Average		2546	0.166
T_1	Average of curve fitting to T_1 data[d]		4966	0.169
	Using R from T_2 data		4975	0.166

[a] The expected χ^2 for fitting these forms to the T_2 data was 20 ± 7 so it is seen that all forms fit the data well though the linear form is least favored.
[b] Background and R computed for the wider-pulse-height region corresponding to the triton peak of T_1.
[c] For T_2 the fits were to regions excluding the recoil-triton peak.
[d] For T_1 the fits were to the entire spectrum above 1.0 MeV. The expected χ^2 was 31 ± 8. All curves fit the data though again the linear form is least favored.

only to variation among the five forms spanned the values obtained.

The same approaches can be used for T_1. However, for this spectrum the count in the valley at ~1 MeV includes a small contribution from the tail of the residual neutron peak. This "spill over" was corrected for on the basis of a fit to the neutron region. The fit need not be precise since the correction to the count in the valley is small. Then the triton peak was fit by approach 2. In this case, since the spectral resolution is dominated by photoelectron statistics the assumption of a Gaussian function for the peak is valid. Alternatively the background subtraction for T_1 was made using the ratio $R=$ (background count/triton count) obtained from T_2. This background was integrated over a region corresponding to the entire triton region of T_1. The results for the two approaches to the T_1 data are also listed in Table IV. They agree very well, though the error is smaller when R is calculated from the T_2 data because the separation of tritons and background is cleaner there. The values of R in this table refer to the correction to the spectrum for T_1. The χ^2 test was satisfied for all curves and for both sets of data. The triton counts corrected for all effects but wall escapes are

$$T_1=4966, \quad T_2=2542.$$

These numbers are based on a total of 6800 observed tritons.

C. Wall Correction

The range of the triton in the standard gas mixture was 6.75 mg/cm^2 or 3.8 mm.[27,36] Thus those tritons which originated close to the walls could escape the gas without leaving their full energy in it. The spectrum of pulse heights for these tritons is weighted toward zero because they tend to lose most of their energy in the wall at the end of their range. In any case, this spectrum is a small, smoothly varying constituent of the time-dependent background. The triton count must therefore be increased by the factor $(1-W)^{-1}$, where W is the fraction of tritons which escape the gas.

On the basis of the Monte Carlo calculation of the stopped muon distribution

$$W=(4.5\pm2.0)\%.$$

The assigned error spans the values calculated from the range of possible assumptions about the parameters in the calculation.

D. Final Triton Count

The final triton counts for the two runs are

$$T_1=5200\pm177, \quad T_2=2660\pm91.$$

The error in T_1 arises from the following: Statistical uncertainty 2.3%, including the statistical error in the random background subtraction and in the calculation of R from the T_2 data, 1.4% for uncertainty in the form of the time-dependent background in T_2 and 2.0% for the wall effect. Combining these in quadrature gives an error of 3.4%. If the quantity R is derived from the T_1 data, the error is 3.8%. For T_2 the errors are 2.2% for statistics, 1.4% for uncertainty in the form of the time-dependent background, and 2.0% for the wall correction. Combining as before the over-all error in T_2 is 3.4%.

V. RESULTS AND DISCUSSION

The resultant rates for runs I and II are 1499 ± 70 sec^{-1} and 1435 ± 75 sec^{-1}, respectively. Combining these two, we have as the result of this experiment

$$\lambda_c=1465\pm67 \text{ sec}^{-1}.$$

Other experimental groups have obtained 1410 ± 150 sec^{-1} (Falomkin *et al.*[10]), and 1505 ± 46 sec^{-1} (Auerbach *et al.*[11]).

Recent predictions of the standard theory are shown in Table V. It would appear that the central value is probably close to 1500 sec^{-1} which is in excellent agreement with all the experiments. The differing calculated values are due to different assumptions about the trion

TABLE V. Predicted He^3 capture rates.

Authors	Rate in sec^{-1}
Wolfenstein[a]	1500
Primakoff[b]	1480
Fujii and Yamaguchi[c]	1550
Drechsler and Stech[d]	1550
Yano[d]	1460
Oakes[d]	1450
Bietti[d]	1530

[a] Ref. 18. [b] Ref. 1. [c] Ref. 15. [d] Ref. 16.

[36] S. K. Allison and S. D. Warshaw, Rev. Mod. Phys. 25, 779 (1953).

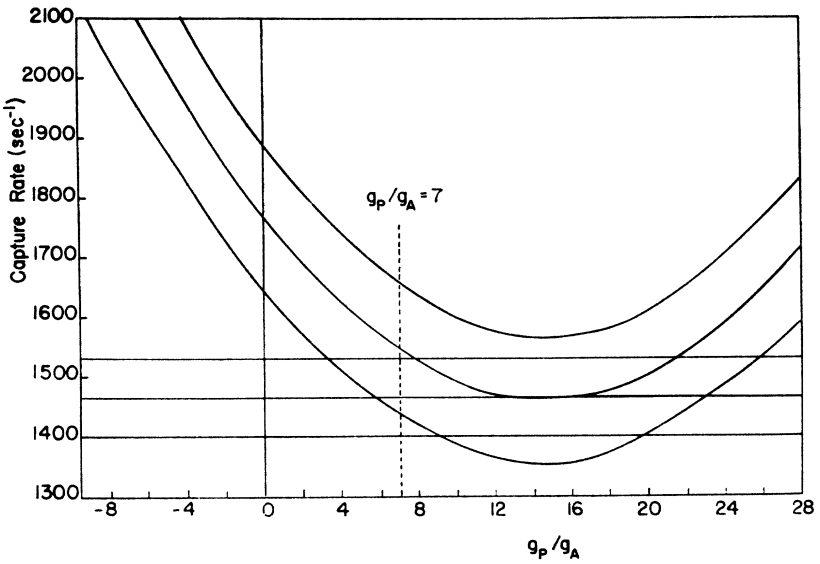

FIG. 11. Variation of capture rate with g_P. The band for the prediction has a spread of ±7% the approximate standard deviation for the theory. The horizontal band is the result of this experiment with its error. The curve is based on the work of Fujii and Yamaguchi (Ref. 15). The overlap is for $4.5<g_P/g_A<24$.

form factors. At the present time the standard deviation in the predicted rate is about 7%. This includes contributions from the following: (1) experimental error in the electron scattering data, and the extrapolation to $q^2\approx m_\mu{}^2$; (2) uncertainties in the ft value in tritium β decay since the calculated values derive from comparison to it; and (3) the uncertainty in the axial-vector and pseudoscalar form factors due to lack of knowledge of the exchange-pion effects. It does not include any uncertainty in g_P. With the considerable effort that is now being made to learn about the trion structure, it is likely that the error in the extrapolated form factors will be reduced and one can hope that the uncertainty in the prediction will be reduced to 4–5%.

If one regards the calculation of g_P/g_A as the chief uncertainty in the standard theory, then a given experiment may be used to evaluate g_P. Figure 11 shows the prediction as a function of g_P and the result of this experiment. Since it happens that the experimental value is close to the minimum possible prediction, the capture rate becomes insensitive to g_P and one can only obtain the broad limits $4.5<g_P/g_A<24$ using the calculation of Fujii and Yamaguchi[15] for example. A somewhat broader range of values is obtained if one starts with the smaller form factors that other authors have obtained. On the other hand, this chance occurrence is advantageous in that very large positive values as well as all negative values of g_P/g_A are ruled out.

Alternatively, we have attempted to set limits on g_V and g_P by combining the result of this experiment with the measurements of capture in hydrogen and of $\pi^+\rightarrow e^++\nu$. Again, the assumption is made of no second class currents and the value of $g_M{}^\mu/g_V{}^\mu$ given by the conserved vector current (CVC) is used. The CVC hypothesis has been well verified in β decay[37] and for the reaction[38]

$$\pi^+\rightarrow\pi^0+e^++\nu$$

(though it has not yet been singled out for measurement in a muon-capture process). From the strictly experimental approach this is the loosest set of assumptions one can make and still obtain good limits on the coupling constants. If, for example, one allows the possibility of second-class terms, in a strict sense there are more constants than can be determined from the experiments to date. Figure 12 shows the curves of constant capture rate which one gets for $g_P{}^\mu/g_A{}^\mu$ plotted

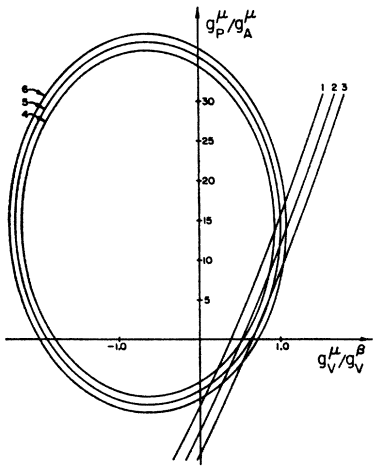

FIG. 12. Curves of constant capture rate. Curves 1, 2, and 3 are for molecular hydrogen capture rates of 410, 450, and 490 sec^{-1}, respectively. Curves 4, 5, and 6 are for He^3 capture rates of 1398, 1465, and 1532 sec^{-1}, respectively. These bands cover the quoted experimental uncertainties only.

[37] T. Mayer-Kuckuk and F. C. Michel, Phys. Rev. **127**, 545 (1962); N. W. Glass and R. W. Peterson, *ibid.* **130**, 299 (1963); Y. K. Lee, L. W. Mo, and C. S. Wu, Phys. Rev. Letters **10**, 253 (1963).

[38] P. De Pommier, J. Heintze, C. Rubbia, and V. Soergel, Phys. Letters **5**, 61 (1963); R. Bacastow, T. Elioff, R. Larsen, C. Wiegand, and T. Ypsilantis, Phys. Rev. Letters **9**, 400 (1962); A. F. Dunaitsev, *et al.*, as reported by I. V. Chuvilo, Brookhaven National Laboratory Report BNL 837 (C-39), 1963 (unpublished), p. 344; D. Bartlett, S. Devons, S. Meyer, and J. Rosen, Phys. Rev. **136**, B1452 (1964); W. Bertram, D. I. Meyer, R. A. Carrigan, Jr., and I. Nadelhaft, *ibid.* **139**, B617 (1965).

as a function of $g_V{}^\mu/g_V{}^\beta$ for μ-molecular hydrogen capture (curves 1, 2, and 3) and for this experiment (curves 4, 5, and 6).[39] The assumed capture rates for curves 1–3 are 410, 450, and 490 sec^{-1}, and for curves 4–6, they are 1398, 1465, and 1532 sec^{-1}, respectively. In each case the band of three curves indicates the spread due to the quoted experimental error only. For the hydrogen experiment other sources of error are small by comparison. For the He^3 experiment we have also considered separately all other sources of error such as form factor uncertainties. There are two regions of intersection of these curves, but if we take only the region which includes the "standard" values, we find

$$0.70<g_V{}^\mu/g_V{}^\beta<1.20$$

and

$$1<g_P{}^\mu/g_A{}^\mu<17.$$

Admittedly, these limits are somewhat uncertain because it is not entirely clear how to combine all the contributing errors. But if a larger experimental number for He^3 is used (somewhere between our number and the one of Ref. 11) or if smaller form factors are used, such as some other authors obtained, the He^3 ellipses become larger and this leads to narrower limits on g_P/g_A. Note that the intersection of the central curves gives

$$g_V{}^\mu/g_V{}^\beta=0.99$$

and

$$g_P{}^\mu/g_A{}^\mu=11.6.$$

Of the many other experiments in muon capture, two in particular,[40,41] the partial capture rates in O^{16} and C^{12}, are compatible with the prediction for $g_P=7g_A$. On the other hand, the radiative muon capture[42] in Cu and Ca and the recent neutron asymmetry experiments[43] in Ca suggest higher values of g_P. In all these cases, however, there is an amount of uncertainty, at present, about the nuclear physics calculations involved.

In conclusion one can say that the present experiment adds to the considerable body of evidence in support of the standard theory of muon capture. There is no evidence of strong weight in contradiction to it, but there are still outstanding problems of great interest, namely, the questions of the second class terms and of the precise value of the pseudoscalar constant.

ACKNOWLEDGMENTS

We wish to thank Professor R. Siegel for his participation in the earlier phases of the experiment. We have benefitted greatly from many clarifying discussions with Professor L. Wolfenstein. Our technicians, G. Burtner and D. Beatty, played an important role both in preparing and running the experiment. D. Hall and M. O. Larson helped with analysis of the data.

APPENDIX

The timing system is such that the data fit the curve

$$\mu\frac{dN}{dt}=(1-F)(e^{-Dt_D})\left[A\lambda e^{-\lambda t}\left(1+\frac{BC}{A\lambda}\right)+B(1-C)\right].$$

The symbols are defined as follows:

A—Integrated time-dependent count for one of the delayed event detectors;
B—Random-background rate for this detector;
C—Fraction of μ pulses which give rise to time-dependent delayed events of all three types;
D—Random-background rate summed over the three types of data.
λ—Muon-disappearance rate;
t_D—Dead time in the delayed-event circuitry, in this case 25 μsec;
μ—Number of muon gates in the run;
F—Probability for accidental anticoincidence due to $\bar{2}$ in any delayed event. $F=0.05$.

Where ratios of integrated counts are taken within one run or for runs with similar counting rates the factors in front of the bracket cancel. Notice that the amplitude of the time-dependent term includes a contribution from the random background. This and the factor $(1-C)$ stem from the fact that only the first count to get through the μ gate is processed. This from also applies to a single pulse-height region if it is understood that A and B refer to this region only.

For the standard run this effect gave rise to a correction to the electron count of -0.2%. For the efficiency and "pure Xe" runs the correction was entirely negligible. This correction played no role in calculating the triton count through it made for a 2% correction to the time-dependent background under the triton peak. The only place this effect played a significant role is in the residual slow neutron associated peak in the pulse-height spectrum for T. Here the expected neutron event count in the time-dependent curve is 9% of the triton count for either the T_1 or T_2 data. The remaining neutron count after this correction is 14% of the triton count in each case.

---

[39] For the He^3 curves the form factors and other constants of Ref. 15 were used. We assume from Ref. 7 that $g_A{}^\mu=g_A{}^\beta$. For the hydrogen capture curves we took $g_A{}^\beta/g_V{}^\beta=1.19\pm0.03$.

[40] R. Cohen, S. Devons, and A. Kanaris, Nucl. Phys. **57**, 255 (1964); A. Astbury *et al.*, Nuovo Cimento **33**, 1020 (1964).

[41] E. J. Maier, R. M. Edelstein, and R. T. Siegel, Phys. Rev. **133**, B663 (1964).

[42] W. T. Chu, I. Nadelhaft, and J. Ashkin, Phys. Rev. **137**, B352 (1965); M. Conversi, R. Diebold, and L. di Lella, *ibid.* **136**, B1077 (1964).

[43] V. S. Evseev, V. S. Roganov, V. A. Chernogorova, Chang Run-Hwa and M. Szymczak, Phys. Letters **6**, 332 (1963); E. W. Anderson and J. E. Rothberg, Bull. Am. Phys. Soc., **10**, 80 (1965).